# Chapter 5
# Material characterization of unbound granular layers

## 5.1 Introduction

Aggregates and soil, treated as unbound granular materials (UGMs) are used in base, subbase, and subgrade layers of the asphalt pavement, serving a crucial role in load distribution. The shear resistance of aggregate skeleton through interlocking of particles gives bearing capacity to UGMs. With the growing demands on pavement loading and performance, it becomes increasingly vital to deepen our fundamental comprehension of mechanical behaviour of UGMs and their response to loading.

## 5.2 Mechanical behaviour of UGMs

The scientific use of suitable materials in pavement layers requires either pre-existing knowledge of their effective performance (using empirical relationships along with index testing) or the facility to measure and forecast their performance. The mechanical properties of materials can be determined using apparatus as mentioned in later section (refer to section 4.3). Mainly fundamental data (stress-strain response, load-deformation response) are required from these tests so that a comprehensive understanding of the material's behaviour can be made [236]. In the context of this dissertation, the term 'mechanical (fundamental) behaviour' is used to denote the failure behaviour (strength), the elastic deformation behaviour (stiffness), and the irreversible deformation behaviour.

Materials subjected to repeated loading conditions (significantly below the failure/yield stress level), experience both recoverable and non-recoverable deformation components.

Figure 5.1 depicts the plastic (nonrecoverable) and elastic (recoverable) strain components under repeated loading conditions.

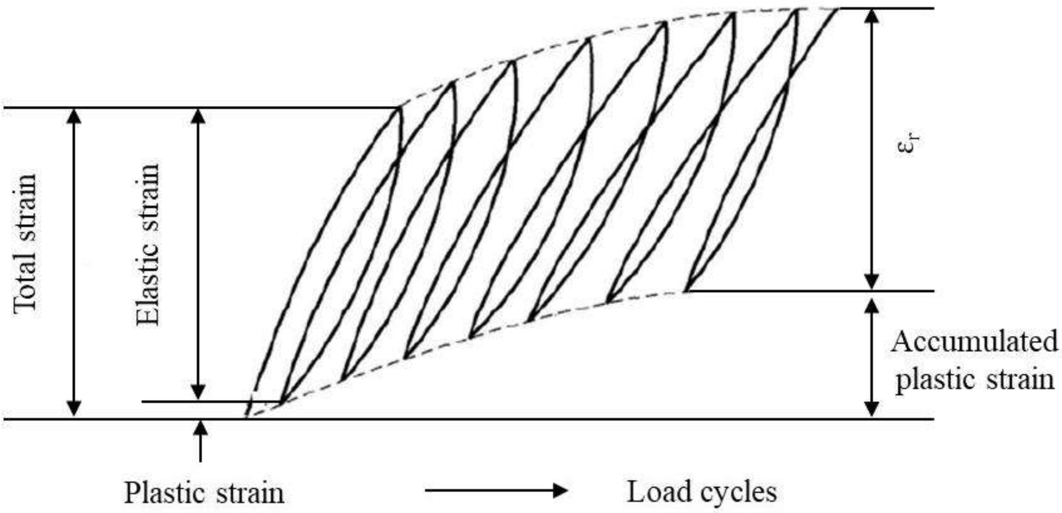


**Figure 5.1.** Strain in material under repeated load test [16].

As shown in Figure 5.1, granular materials experience some non-recoverable deformations after each load application and hence it cannot be considered as truly elastic material [237]. Past studies [238] show that several factors like applied stress, moisture content, material density, aggregate gradation, state of stress, load repetitions, and frequency affect resilient behaviour of unbound granular materials. The most significant parameter was identified as state of stress. Aggregates in base and subbase layers exhibits stress hardening characteristics whereas fine-grained soil in subgrade layer show stress softening behaviour.

### 5.3 Non-linear stress dependent material behaviour of UGM

The elastic characteristics of a material are traditionally defined by the theory of elasticity, using the modulus of elasticity, E, and Poisson's ratio, ν. When it comes to unbound granular layers (UGLs), the elastic modulus E is substituted with the resilient modulus, which describes the stress-dependent elastic (or recoverable) behaviour of a material under repeated loading. Hveem first observed the resilient properties of UGMs, concluding that the deformation of these materials under transient loading is elastic that can be recovered [239]. The concept of the resilient modulus was later introduced by Seed et al. [240] to characterize the elastic response of subgrade soils and their relation to fatigue failures in asphalt pavements.

While granular materials are not entirely elastic [237], they do undergo some non-recoverable deformation with each load application. In the case of transient loads, and after the initial few load applications, the increase in non-recoverable deformation is significantly smaller compared to the resilient/recoverable deformation, as shown in Figure 5.2.

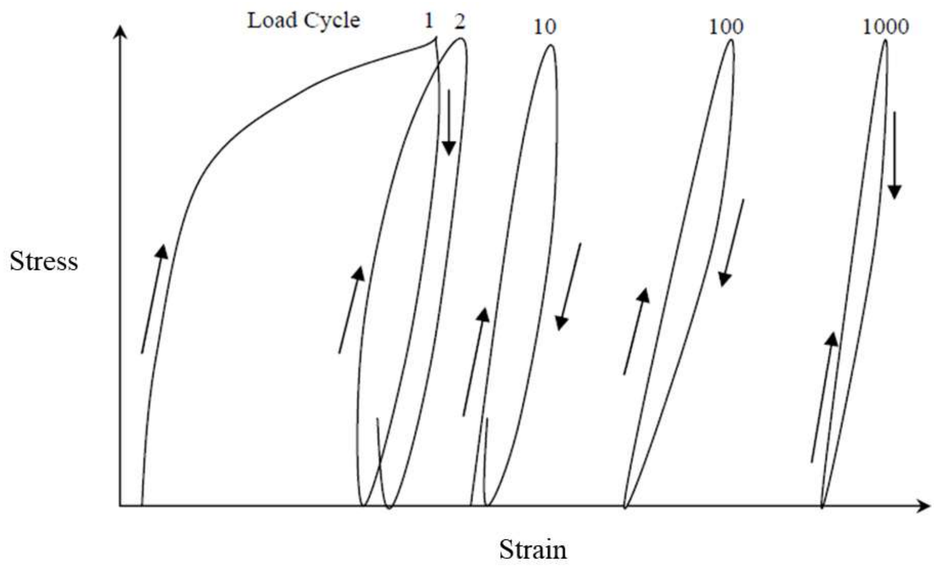


**Figure 5.2.** Behaviour of granular materials under repeated loading [241].

The term "resilient" denotes the segment of energy that is invested into a material during loading and is fully restored upon unloading [242]. This resilience exhibited by granular layers forms the primary basis for introducing elastic theory to examine material response to loading. The engineering parameter typically used to describe this behaviour is the resilient modulus ($M_r$). Stress dependent behaviour of materials used in unbound granular layers are generally evaluated using resilient modulus ($M_r$) test [243]. It represents elastic stiffness properties of the pavement materials. Resilient modulus is the ratio of deviatoric stress ($\sigma_d$) to recoverable strain ($\varepsilon_r$) as shown in Eq. 5.1.

$$M_r = \frac{\sigma_d}{\varepsilon_r} \tag{5.1}$$

Resilient behaviour of unbound aggregates in base and subbase layer and soil in subgrade layer are evaluated using repeated load triaxial compression testing in laboratory. The $M_r$ of unbound granular base materials and fine-grained subgrade soils is well-known to depend on the current state of stress experienced by each pavement layer element. Since stress states vary within a layer, the moduli also change with depth and horizontal distance. Consequently, it is essential to predict layer modulus distributions as a function of stress states for accurate pavement mechanistic analysis. This approach yields modulus distributions that align with stress distributions or stress bulbs within the layer, which significantly differ from the simplistic single modulus assignment used in linear elastic layered solutions. Moreover, relying solely on a single modulus assignment can lead to the prediction of large horizontal tensile stresses in aggregate base layers, which contradicts the limited tensile capacity of aggregate materials. Efforts has been made to develop models that can best describe the non-linear stress dependent behaviour of UGMs. Following section discusses few widely used models starting from oldest to most advanced and recent developments considering material anisotropy.

### 5.3.1 K-θ model

The k-θ model, initially proposed by Seed et al. [240] is a non-linear stress dependent power function model. The stiffness value of UGM was determined by Brown and Pell [57] using pulse load test on a pavement built as a test section. The evaluated $M_r$ values were plotted against bulk stress also known as first stress invariant (θ) on a logarithmic scale. The relation was observed as a straight line as shown in Figure 5.3. This method of presenting non-linear stress dependent properties of UGMs is now considered as a standard method in pavement engineering. This well-known k-Θ model is given as:

$$M_r = k_1 \Theta^{k_2} \tag{5.2}$$

where $M_r$ is resilient modulus, $\Theta = \sigma_1 + \sigma_2 + \sigma_3$ = bulk stress, and $k_1$ and $k_2$ are material constant.

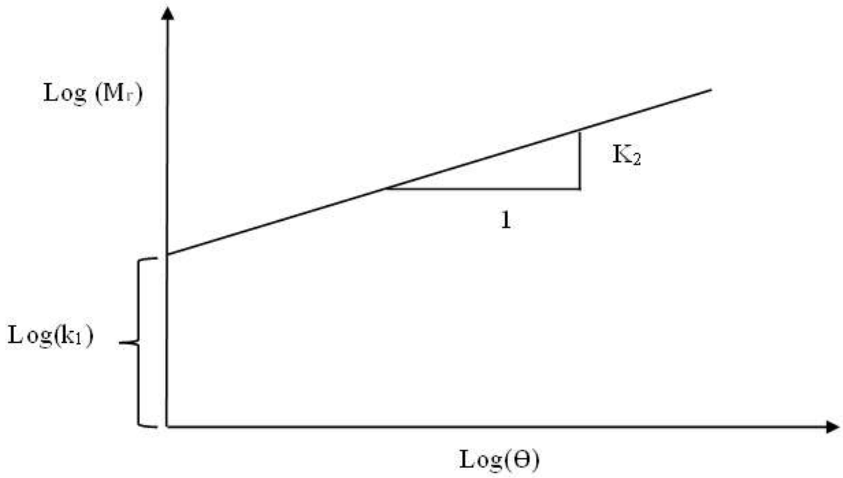


**Figure 5.3.** Variation of resilient modulus with bulk stress.

The k-Θ model is widely used in pavement engineering to account for the stress dependency of the resilient modulus. Its simplicity and practical utility make it a valuable tool for analysing material stiffness under varying stress conditions. However, the model has some drawbacks [244,245]. Firstly, it considers stress levels in the materials solely based on bulk stress parameter. It means that all combinations of principal stresses which sums to same value of bulk stress will have same effect on the resilient modulus. It does not consider individual effect of confining stress and deviator (shear) stress. Secondly, the model often assumes a constant Poisson's ratio when calculating radial strain in test samples. However, earlier research [244,246,247] highlights that Poisson's ratio varies with applied stresses. Practically, materials in unbound granular layers are subjected to axial stress (due to tire loading), confining stress (due to materials around it), and shear stress (due to moving action of load) as shown in Figure 5.4.

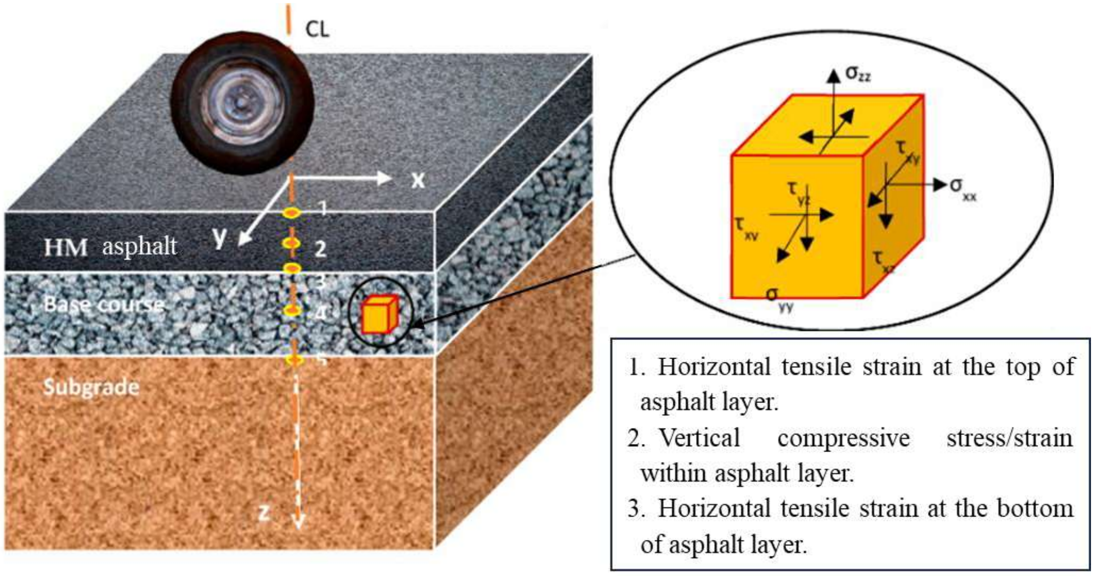


**Figure 5.4.** Stresses in unbound UGMs and point of interest in pavement analyses [248].

The base layer as shown in Figure 5.4 is representative layer of granular aggregate layers and points marked in this diagram represents location or region of interest for researchers in pavement analyses. These points have been explained in detail in Chapter 6.

### 5.3.2 Uzan model

The Uzan model [245] considers the effect of both deviatoric stress as well as confining stress to represent changes in resilient modulus with state of stress in unbound aggregate base layers. The Uzan model [245] is particularly useful for predicting the stress-hardening behaviour of unbound aggregate materials in axisymmetric finite element (FE) analyses as given by Eq. 5.3. Considering these stress conditions, the Uzan model provides valuable insights into the mechanical response of pavement materials subjected to repeated loading. Researchers have successfully applied this model to characterize the nonlinear elastic behaviour of unbound aggregates in laboratory testing, demonstrating its practicality for flexible pavement analysis.

$$M_r = k_1 \left(\frac{\theta}{p_o}\right)^{k_2} \left(\frac{\sigma_d}{p_o}\right)^{k_3} \tag{5.3}$$

where, $\theta$ is bulk stress ($\sigma_1$+$\sigma_2$+$\sigma_3$ = $\sigma_1$+2$\sigma_3$), $\sigma_d$ is deviator stress ($\sigma_1$-$\sigma_3$), $\sigma_1$ is axial stress, $\sigma_3$ is confining stress, $p_o$ is unit pressure, and $k_1$, $k_2$, $k_3$ are constants obtained from multiple regression analysis of repeated load triaxial compression test data.

### 5.3.3 Universal octahedral shear stress model

In subsequent work, Witczak and Uzan [49] introduced a universal model based on the Uzan model [245]. In this modified approach, the deviator stress term was replaced with the octahedral shear stress (see Eq. 5.4). Notably, the universal octahedral shear stress model accounts for material characteristics in all three spatial directions (x, y, and z). As a result, this model is particularly well-suited for three-dimensional finite element (FE) pavement analysis.

Earlier, the Uzan model played a crucial role in understanding the resilient behaviour of pavement materials. By incorporating shear stress effects, it addressed limitations present in earlier models. The universal model considers octahedral shear stress and provides valuable insights for 3D FE analyses of asphalt pavements. The ability to consider material's behaviour in multiple directions makes it suitable for realistic pavement simulations.

$$M_r = k_1 p_a \left(\frac{I_1}{p_a}\right)^{k_2} \left(\frac{\tau_{oct}}{p_a}\right)^{k_3} \tag{5.4}$$

$$I_1 = \theta = \sigma_1 + \sigma_2 + \sigma_3$$

$$\tau_{oct} = \frac{1}{3}[(\sigma_1 - \sigma_2)^2 + (\sigma_2 - \sigma_3)^2 + (\sigma_1 - \sigma_3)^2]^{\frac{1}{2}}$$

where, $p_a$ is atmospheric pressure, $\tau_{oct}$ is octahedral shear stress, $I_1$ is first stress invariant, and $k_1$, $k_2$, $k_3$ are constants obtained from multiple regression analysis of repeated load triaxial compression test data.

### 5.3.4 NCHRP model

The NCHRP model was introduced in the Mechanistic Empirical Pavement Design Guide (MEPDG) to evaluate $M_r$ using a generalized constitutive model similar to universal octahedral shear stress model as given in Eq. 5.5. In the MEPDG software, there are three input levels for the materials and traffic based on the importance of the project and availability of data. In level I analysis, $M_r$ is determined through laboratory testing while in level II analysis, it is determined through the correlations with some other material properties like CBR value. In level III analysis, typical default values of layer modulus as a function of soil classification are selected from the database of highway agencies [249]. The NCHRP model is used to model nonlinear stress dependent response of UGMs (aggregates and soil) for level I analysis. The constitutive equation for evaluating $M_r$ used in MEPDG design guidelines is given as:

$$M_r = k_1 p_a \left(\frac{\theta}{p_a}\right)^{k_2} \left(\frac{\tau_{oct}}{p_a} + 1\right)^{k_3} \tag{5.5}$$

where, $p_a$ is atmospheric pressure and all other terms have their usual meaning as discussed earlier.

### 5.3.5 Bilinear model

The resilient modulus of fine-grained soil typically exhibits stress-softening behaviour. It means, as stress in the material (fine grained soil) increases, $M_r$ is found to decrease. This kind of material behaviour are represented by constituting a suitable relationship between resilient modulus and deviator stress. The bilinear model proposed by Thompson and Robnett [64] is widely used for a fine-grained soil used in subgrade layer. This model is expressed as follows:

$$M_r = k_1 + k_3(k_2 - \sigma_d) \qquad when\ \sigma_d \leq k_2$$
$$M_r = k_1 - k_4(\sigma_d - k_2) \qquad when\ \sigma_d \geq k_2 \tag{5.6}$$

where, $\sigma_d$ is deviator stress and $k_1$, $k_2$, $k_3$, and $k_4$ are material constants obtained from regression analyses. In bilinear model, the parameter $k_1$ is termed as breakpoint modulus and it is considered as characteristic property of soil. An illustrative example of these constants in Bilinear model is shown in Figure 5.5.

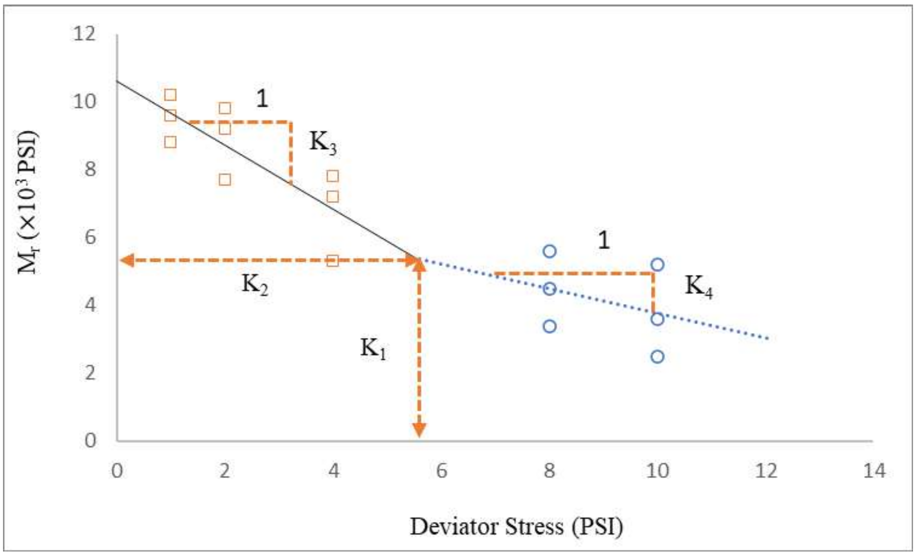


**Figure 5.5.** Model constants in Bilinear model.

As the name itself suggests, Bilinear model is a combination of two linear relations between $M_r$ and $\sigma_d$. The point where slope of the $M_r$-$\sigma_d$ line changes, is termed as breakpoint modulus also known as $k_1$.

## 5.4 Material selection and properties

Locally available materials (soil and aggregates) were used in this study for different layers of base, subbase, and subgrade of the asphalt pavement. For subgrade layer, five different types of soil (red soil of two different sources, fly-ash soil, fine-grained cohesive soil, and black cotton soil) were used to understand its effect on pavement response. A single layer of granular subbase (GSB) has been used in this study as per the guidelines of IRC:37 [20], a single drainage cum filter layer with GSB gradations V and VI as per MoRTH [216] specifications were selected. Wet mix macadam (WMM) was selected as base layer as it widely used across the country for asphalt pavement construction. Physical requirements and aggregate gradations of the materials are discussed in following section.

The suitability of materials selected for various layers are checked as per the MoRTH [216] specifications. Some test standards like aggregate impact value, liquid limit, plasticity index, and CBR value has been specified for aggregates to be used as subbase layer. Standard limits of Los Angeles abrasion value or aggregate impact value, and combined flakiness and elongation index has been specified for materials to be used in WMM layer. For soil used in subgrade layer, it shall meet the free swelling index, dry density, and design CBR value criteria as specified by MoRTH [216].

### 5.4.1 Physical properties of soil

The materials used in subgrade layer can be soil, moorum, gravel, fly ash, pond ash, or a mixture of these. Red soil locally available from two different sites, fine grained cohesive soil, black cotton soil, and silty soil mixed with fly ash was used in this study. The size of the coarse material in the soil shall not exceed 50 mm to avoid any difficulty in placement and compaction of fill material. All the materials were sieved through 4.75 mm IS sieve before conducting any physical test. Maximum laboratory dry unit weight shall not be less than 17.5 kN/m$^3$ as specified in MoRTH [216]. These soils have first been categorized based on liquid limit and plasticity index as specified in IS 1498 [250] as shown in Table 5.1. The physical requirement as per the MoRTH [216] specifications and test results obtained are summarised in Table 5.2. Generally, locally available soil material is used for the construction of embankment and subgrade layer. The properties of soil vary in a small stretch of pavement section which do not permit to impose stringent physical properties requirement on soil. As per MoRTH [216] specifications, maximum dry weight and sweeling characteristics of soil is tested.

**Table 5.1.** Soil classification based on liquid limit and plasticity index

| Soil | Liquid limit (%) | Plastic limit (%) | Plasticity index (%) | Soil classification (IS 1498) |
|---|---|---|---|---|
| Red soil - 1 | 36.24 | 26.14 | 10.10 | MI |
| Red soil - 2 | 32.60 | 24.48 | 8.12 | ML |
| Fly-ash soil | 33.98 | 18.78 | 15.20 | CL |
| Cohesive soil | 42.64 | 27.18 | 15.46 | CI |
| Black cotton soil | 47.53 | 20.93 | 26.60 | CH |

**Table 5.2.** Physical properties of soil

| Soil type | Parameters | Test protocol | Test results | Specification limit |
|---|---|---|---|---|
| Red soil 1 | Size | MoRTH | < 4.75 mm | Max 50 mm |
| | Max. dry unit wt. | IS 2720: Part 8 | 18.60 kN/m$^3$ | 17.5 kN/m$^3$ |
| | Free swelling index | IS 2720: Part 40 | Non-expansive | < 50% |
| Red soil 2 | Size | MoRTH | < 4.75 mm | Max 50 mm |
| | Max. dry unit wt. | IS 2720: Part 8 | 18.75 kN/m$^3$ | 17.5 kN/m$^3$ |
| | Free swelling index | IS 2720: Part 40 | Non-expansive | < 50% |
| Cohesive soil | Size | MoRTH | < 4.75 mm | Max 50 mm |
| | Max. dry unit wt. | IS 2720: Part 8 | 18.80 kN/m$^3$ | 17.5 kN/m$^3$ |
| | Free swelling index | IS 2720: Part 40 | 12% | < 50% |
| Fly ash soil | Size | MoRTH | < 4.75 mm | Max 50 mm |
| | Max. dry unit wt. | IS 2720: Part 8 | 17.82 kN/m$^3$ | 17.5 kN/m$^3$ |
| | Free swelling index | IS 2720: Part 40 | Non-expansive | < 50% |
| Black cotton | Size | MoRTH | < 4.75 mm | Max 50 mm |
| | Max. dry unit wt. | IS 2720: Part 8 | 18.40 kN/m$^3$ | 17.5 kN/m$^3$ |
| | Free swelling index | IS 2720: Part 40 | 44% | < 50% |

As per MoRTH specifications, when an expansive soil having free swelling index value, less than 50% is used as fill material, subgrade soil shall be non-expansive in nature. In this study, non-expansive fill material has been assumed; so, a free swelling index of 44% for black cotton soil in subgrade layer should be acceptable.

### 5.4.2 Physical properties of aggregates

The physical requirements of aggregate materials for granular base and subbase layers are different. Aggregates used in granular subbase layer is tested for aggregate impact value, liquid limit, plasticity index, and CBR value at 98% of dry density while aggregates used in granular base layer is tested for Los Angeles abrasion value or aggregate impact value and combined flakiness and elongation index value. Since single drainage cum filter layer has been used as granular subbase in this study, so grade V and VI as per MoRTH [216] guidelines were selected in the study. The physical requirements and test results of the aggregate material for granular subbase layer is summarised in Table 5.3. The physical properties of aggregates in unbound base layer can be obtained from Table 4.2 (Chapter 4).

**Table 5.3.** Specification limits and physical properties of aggregates for subbase layer

| **Properties** | **Impact value** | **Liquid limit** | **Plasticity** | **CBR value** |
|---|---|---|---|---|
| Specification limit | Max. 40% | Max. 25% | Max. 6 | Min. 30% |
| Test protocol | IS 2386-Part 4 | IS 2720-Part | IS 2720-Part 5 | IS 2720-Part |
| Test result | 14.6% | 3.4% | 3.4% | 46% |

The physical requirements of aggregates used in granular subbase layer were found well within the specified limit. Plastic limit of the aggregate fines (passing 425 micron IS sieve) was found to be zero as it was not possible to make 3 mm diameter thread.

In this research, Granite (a siliceous aggregate) was used for the preparation of granular subbase and base samples. It is a hard crushed stone with specific gravity of nearly 2.7 generally used for the preparation of base and asphalt concrete layer. It has good toughness and crushing strength value. As shown in Table 5.3, Granite aggregates possess good impact resistance and abrasive resistance. It has relatively lower water absorption (0.2% in this study) and high CBR value. After the physical test, aggregate gradation was done for grade V and grade VI of granular subbase as shown in Figure 5.6 and Figure 5.7 respectively and wet mix macadam as shown in Figure 5.8. Mid-point gradation was selected as target gradation in this study for testing materials.

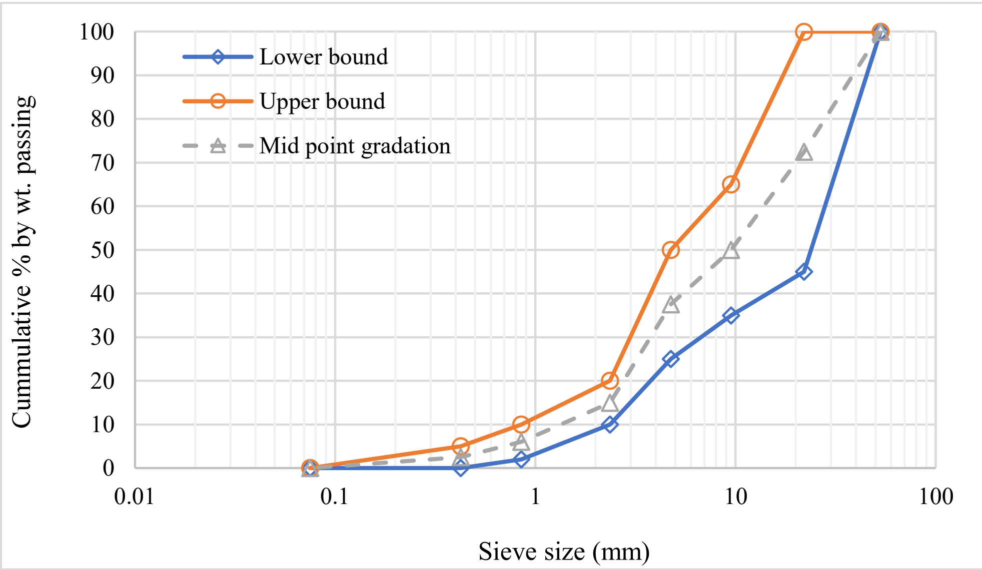


**Figure 5.6.** Aggregate gradation for granular subbase grade V.

Since these aggregates were further used for resilient modulus test in which 100 mm diameter mold is used so aggregate size higher than 22 mm was discarded and these proportion of aggregates were adjusted by aggregate size finer than 22 mm. An accepted rule of thumb is that the mold diameter should be at least four times the maximum aggregate size [251].

Granular subbase grading V and VI are well graded aggregate structure in which almost every size of aggregate starting from 26.5 mm to 75 micron is present. Since, every size of particles is present in these grades of granular subbase, it allows to be used as filter cum drainage layer. Fine particles act as barrier to the intrusion of soil from the subgrade layer just below it and coarser particles allow drainage of water through it.

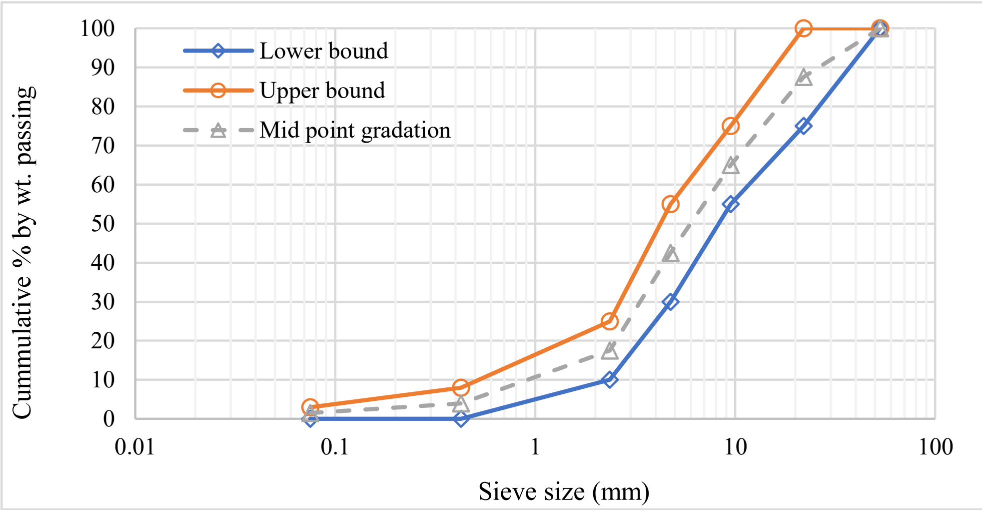


**Figure 5.7.** Aggregate gradation for granular subbase grade VI.

As shown in Figure 5.7, grade VI subbase aggregate contains 17.5% fine aggregate (passing 2.36 mm IS sieve) marginally higher than the grade V aggregates (15% fine aggregate).

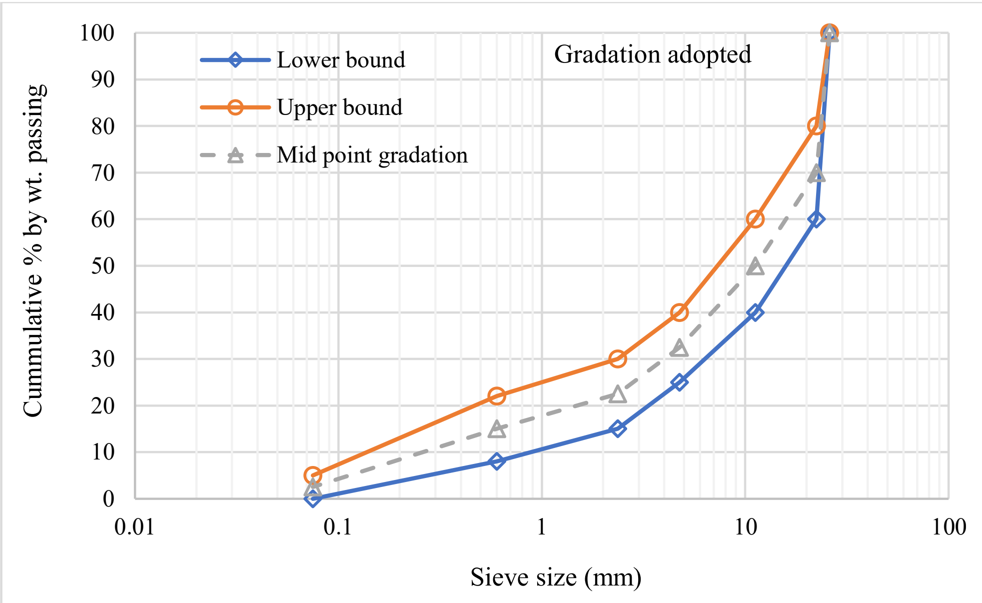


**Figure 5.8.** Aggregate gradation for wet mix macadam.

The maximum size of aggregate in wet mix macadam (WMM) as specified in MoRTH is 45 mm. As explained earlier, the diameter of mold should be at least four times the maximum aggregate size; so, these aggregates were discarded, and same fraction was adjusted to 22.4 mm IS sieve. So, adopted gradation is different than gradation obtained using aggregate size as specified in MoRTH [216]. WMM is composed of a higher percentage of coarse aggregates (77.5% retained on 2.36 mm IS sieve) and lesser fraction of fine aggregates (22.5% passing 2.36 mm IS sieve). The base layer (WMM) was also stabilized with bitumen emulsion to study the effect of base layer stabilization on the structural response of asphalt pavement. The idea of stabilization was to see if thickness of asphalt layer can be reduced compared to the one used with conventional WMM base layer. Since the asphalt layer is the costliest one in asphalt pavement construction due to the presence of bitumen; so, reduction in asphalt layer thickness can be an economical option. However, cost benefit analysis is beyond the scope of this study. Further stabilization of the base improves its stiffness; so, it allows for higher load carrying capacity. Therefore, the effect of base stabilization on overloading leverage was also studied. Properties of stabilized base material are discussed in the following section.

### 5.4.3 Properties of emulsion treated stabilized base

Emulsion treated aggregate (ETA) is a cold mix base layer stabilization technique in which recycled aggregates or virgin aggregates are treated with slow-setting (SS) asphalt emulsion [252–254]. The application of bitumen emulsion in stabilizing aggregate base material is considered as an environmentally sustainable and cost-effective alternative. Presence of bitumen emulsion improves cohesive strength and reduces moisture susceptibility of the virgin aggregate material [255]. Past researchers [256] have reported increase in shear strength, resilient modulus and rutting performance of the treated aggregates. ETA is gaining popularity in India as it significantly improves cohesion and moisture resistance due to the presence of thin bituminous film around the aggregates. The gradation of the aggregate used in this research is shown in Figure 5.9, whereas other technical details of ETA are shown in Table 5.4. There is no unified laboratory method for the design ETA; so various highway agencies are using different mix design methods in different countries. In this research, the optimum fluid content (OFC) required for preparing the ETA mix was estimated as per the IRC guidelines [258]. The SS-2 emulsion type, 4% by weight of the mix and 1% cement as the active filler was used to stabilize the aggregate base layer. The $M_r$ value of ETA was obtained using the IT pulse modulus test [217].

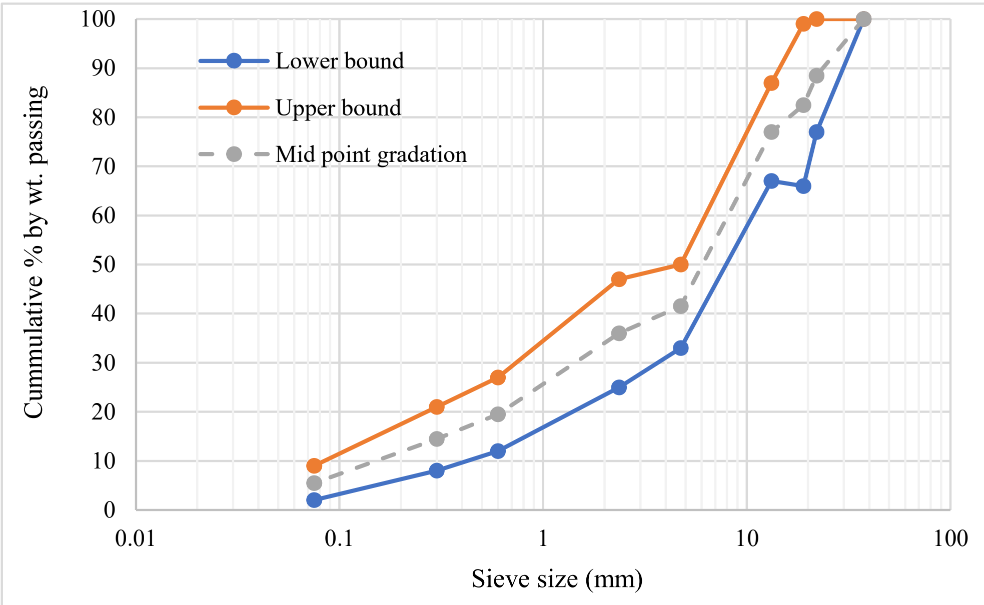


**Figure 5.9.** Aggregate gradation adopted for emulsion treated stabilised base.

As shown in Figure 5.9, the fine aggregates (< 2.36 mm) in ETA constitutes 36% of the total weight which is significantly higher than in case of SMA-1 and SMA-2 (only 20%). However, BC mixes, specifically BC-2, have higher fine aggregate content (50%) than other asphalt mixes and ETA. Details of $M_r$ test for bound layer are provided in previous chapter (See Chapter 4, section 4.3.1.5), for unbound granular layers, $M_r$ test procedure and results are discussed in next section.

**Table 5.4.** Emulsion treated aggregate mix properties

| ETA properties | Obtained values | Guidelines/Test protocol |
|---|---|---|
| Optimum fluid content | 6.4% | IRC: 37-2012 [259] |
| Maximum dry density | 2.12 g/cm$^3$ | IRC: 37-2012 [259] |
| Emulsion type | SS-2 | IS: 8887-2018 [260] |
| Emulsion dosage | 4% | IRC: 37-2012 [259] |
| Cement content | 1% | IRC: 37-2012 [259] |
| ITS (14 days) | 232 KPa | ASTM: D6931 [261] |
| $M_r$ at 35° C | 860 MPa | ASTM: D4123 [217] |

## 5.5 Resilient modulus test using triaxial compression testing

Resilient modulus is the ratio of the amplitude of the repeated axial stress to the amplitude of the recoverable axial strain. It provides basic relation between stress and deformation of granular materials for the structural analyses of layered pavement structure. Pavement materials like subgrade soil and aggregate materials used in base and subbase layer can be characterized using $M_r$ test. The materials under triaxial testing are subjected to mainly axial and confining stresses as shown in Figure 5.10.

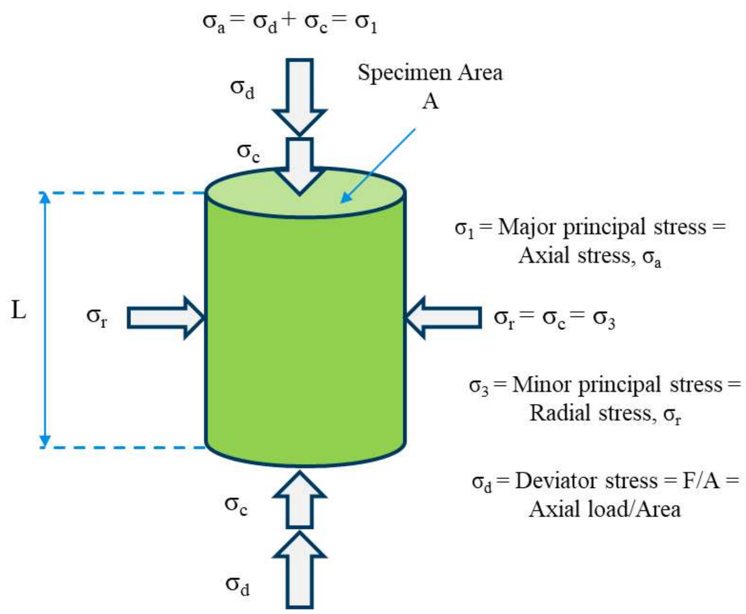


**Figure 5.10.** Stresses in materials under triaxial compression testing.

$M_r$ test is conducted on optimum moisture content (OMC) using a cylindrical sample of 100 mm diameter and 200 mm height. The realistic condition of pavement materials subjected to moving tire load can be simulated using this test by changing the state of stress in the material. $M_r$ of an unbound granular material is determined using repeated load triaxial compression testing in which a haversine load pulse of duration 0.1 sec is applied.

### 5.5.1 Determination of OMC

Firstly, the relation between water content and dry density is established using heavy compaction as specified in IS 2720 part 8 [262]. A suitable quantity of test material is taken in a 1000 $cm^3$ capacity mold. The sample is mixed thoroughly with a trial amount of water and compacted in five equal layers; each layer being given 25 blows from the 4.9 kg rammer dropped from a height of 450 mm. The mold with material is weighed. This process is repeated with increased amount of water in each trial till weight of the mold with material starts decreasing. The OMC corresponds to the maximum dry density of the sample. Dry density of the sample is computed using following relation:

$$\gamma_d = \frac{\gamma_m}{100 + w} \times 100 \tag{5.7}$$

where, $\gamma_d$ is dry density of the sample, $\gamma_m$ is the bulk density of the test specimen, and $w$ is water content of the material in percent.

### 5.5.2 Determination of resilient modulus

Sample is prepared as per the guidelines of IS 2720 part 8 [262] mentioned in previous section. The compacted sample at OMC as shown in Figure 5.11 is placed in triaxial compression chamber. Porous bronze disc and specimen cap is placed at the top surface of the sample. The cylindrical sample is enclosed by an elastic rubber membrane to keep it integrated and avoid any material coming out in the chamber. The membrane is then sealed tightly against the cap with the O-ring. Once the test set up in triaxial chamber is completed, it is connected with the pressure supply line for applying desired confining pressure.

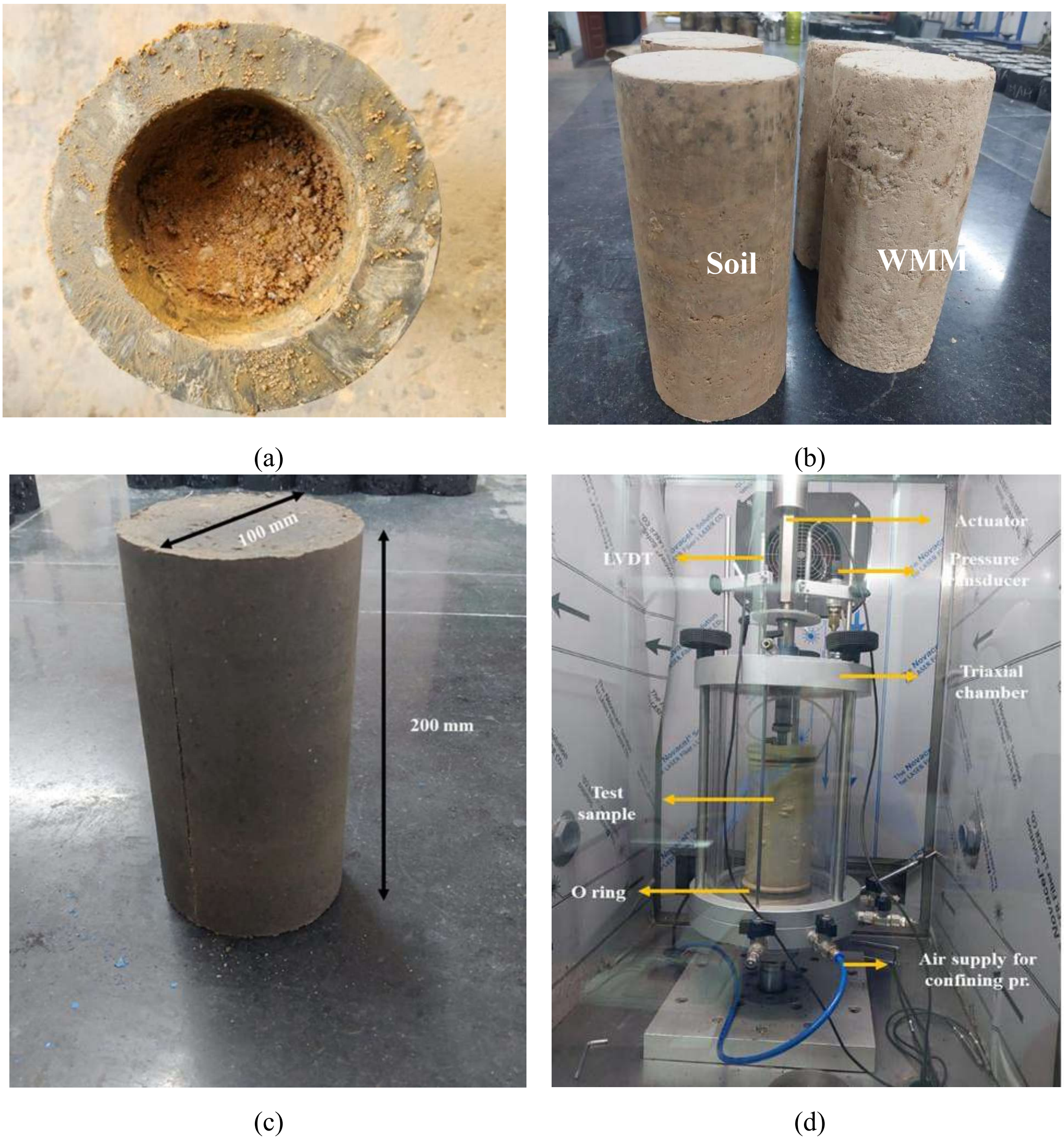


**Figure 5.11.** (a) OMC/MDD determination (b) Compacted samples of soil and aggregates (c) Sample dimensions (d) Triaxial compression test set up.

A repeated axial cyclic stress of load duration 0.1 sec is applied to a cylindrical specimen. Test is conducted using dynamic cyclic stress and a static confining stress provided by triaxial compression chamber as specified by AASHTO T-307 [263]. The sample response in terms of total axial recoverable deformation is measured using linear variable differential transducer (LVDT) to determine the resilient modulus.

Air is used to produce confining stress in the triaxial compression chamber. The haversine shaped load pulse of duration 0.1 sec and rest period of 0.9 sec is applied to the test sample. Deformation measuring system consists of two LVDTs fixed to opposite sides of actuator outside the test chamber as shown in Figure 5.12 (detailed view of test set up). These two LVDTs are located equidistant to the actuator.

Resilient modulus test is started by applying 500 repetitions of load cycles equivalent to a maximum axial stress of 27.6 kPa and corresponding cyclic stress of 24.8 kPa in case of soil and set confining pressure to 103.4 kPa and cyclic axial stress of 93.1 kPa for base and subbase materials using a haversine load pulse. This loading duration is considered as conditioning period of the test sample. At the end of the conditioning period, if the height of sample is still decreasing, conditioning period is continued to 1000 load cycles. The conditioning of test sample aids in minimizing the effects of irregular surfaces of the specimen.

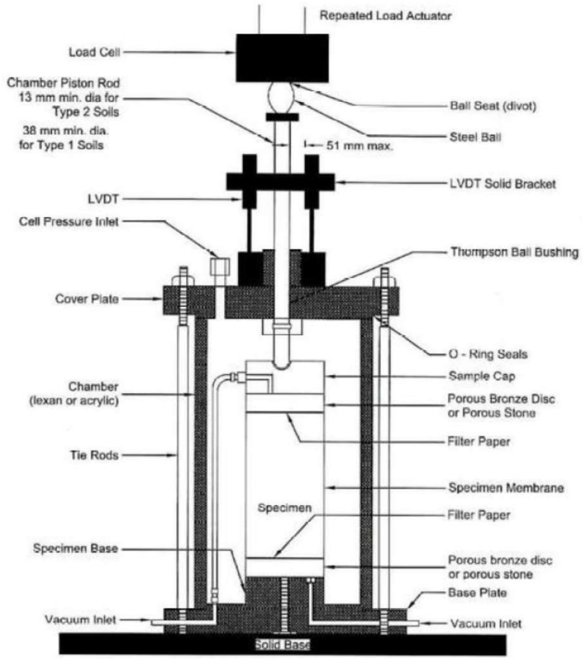


**Figure 5.12.** Triaxial compression chamber with LVDT and load cell [263].

It simulates drained conditions in asphalt pavement system. Details for loading sequence for soil (subgrade layer) are summarized in Table 5.5.

**Table 5.5.** Test sequence and load details for subgrade soil

| Sequence No. | Confining stress (kPa) | Max. axial stress (kPa) | Cyclic stress (kPa) | Contact stress (kPa) | No. of load application |
|---|---|---|---|---|---|
| 0 | 41.4 | 27.6 | 24.8 | 2.8 | 500 |
| 1 | 41.4 | 13.8 | 12.4 | 1.4 | 100 |
| 2 | 41.4 | 27.6 | 24.8 | 2.8 | 100 |
| 3 | 41.4 | 41.4 | 37.3 | 4.1 | 100 |
| 4 | 41.4 | 55.2 | 49.7 | 5.5 | 100 |
| 5 | 41.4 | 68.9 | 62.0 | 6.9 | 100 |
| 6 | 27.6 | 13.8 | 12.4 | 1.4 | 100 |
| 7 | 27.6 | 27.6 | 24.8 | 2.8 | 100 |
| 8 | 27.6 | 41.4 | 37.3 | 4.1 | 100 |
| 9 | 27.6 | 55.2 | 49.7 | 5.5 | 100 |
| 10 | 27.6 | 68.9 | 62.0 | 6.9 | 100 |
| 11 | 13.8 | 13.8 | 12.4 | 1.4 | 100 |
| 12 | 13.8 | 27.6 | 24.8 | 2.8 | 100 |
| 13 | 13.8 | 41.4 | 37.3 | 4.1 | 100 |
| 14 | 13.8 | 55.2 | 49.7 | 5.5 | 100 |
| 15 | 13.8 | 68.9 | 62.0 | 6.9 | 100 |

As shown in Table 5.5, keeping confining stress constant (for five sequence), maximum axial stress was varied to see the variation of $M_r$ with the state of stress in the sample. Contact pressure was kept approximately 10% of the maximum axial stress applied. The conditioning of the sample is terminated if total vertical permanent strain reaches 5%. The possibility of any error during compaction is investigated for excessive deformation in the sample. If no such reason is found, sample is compacted again. Test sequence and loading details in $M_r$ testing of aggregate materials for base and subbase layers are shown in Table 5.6. These materials are used above subgrade layer, which is under higher axial stress, so as to simulate these conditions, a higher confining and maximum stress is applied during $M_r$ test on aggregate materials.

**Table 5.6.** Test sequence and load details for base/subbase materials

| Sequence No. | Confining stress (kPa) | Max. axial stress (kPa) | Cyclic stress (kPa) | Contact stress (kPa) | No. of load application |
|---|---|---|---|---|---|
| 0 | 103.4 | 103.4 | 93.1 | 10.3 | 500 |
| 1 | 20.7 | 20.7 | 18.6 | 2.1 | 100 |
| 2 | 20.7 | 41.4 | 37.3 | 4.1 | 100 |
| 3 | 20.7 | 62.1 | 55.9 | 6.2 | 100 |
| 4 | 34.5 | 34.5 | 31.0 | 3.5 | 100 |
| 5 | 34.5 | 68.9 | 62.0 | 6.9 | 100 |
| 6 | 34.5 | 103.4 | 93.1 | 10.3 | 100 |
| 7 | 68.9 | 68.9 | 62.0 | 6.9 | 100 |
| 8 | 68.9 | 137.9 | 124.1 | 13.8 | 100 |
| 9 | 68.9 | 206.8 | 186.1 | 20.7 | 100 |
| 10 | 103.4 | 68.9 | 62.0 | 6.9 | 100 |
| 11 | 103.4 | 103.4 | 93.1 | 10.3 | 100 |
| 12 | 103.4 | 206.8 | 186.1 | 20.7 | 100 |
| 13 | 137.9 | 103.4 | 93.1 | 10.3 | 100 |
| 14 | 137.9 | 137.9 | 124.1 | 13.8 | 100 |
| 15 | 137.9 | 275.8 | 248.2 | 27.6 | 100 |

Since, fine grained soil exhibits stress softening behaviour so a decreasing value of confining stress is applied; while, aggregate shows stress hardening behaviour, so an increasing confining stress is applied to the sample. Level of confinement in subgrade soil specimen varies from 13.8 kPa to 41.4 kPa while for aggregates in base and subbase layers, it varies from 20.7 kPa to 137.9 kPa. The variation of confining stress, maximum axial stress, and cyclic stress with loading sequence is shown in Figure 5.13 for more clarity.

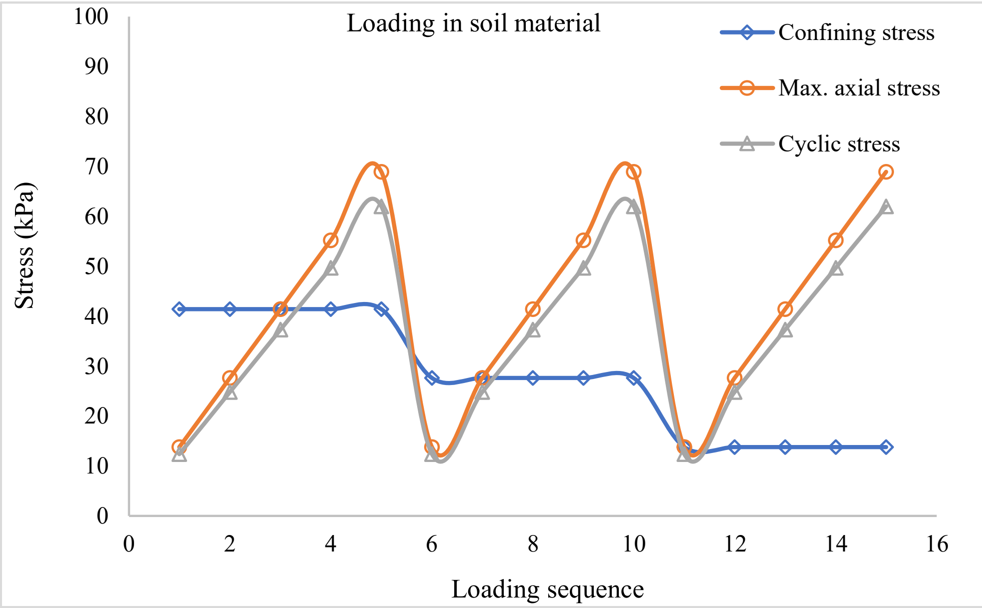


(a)

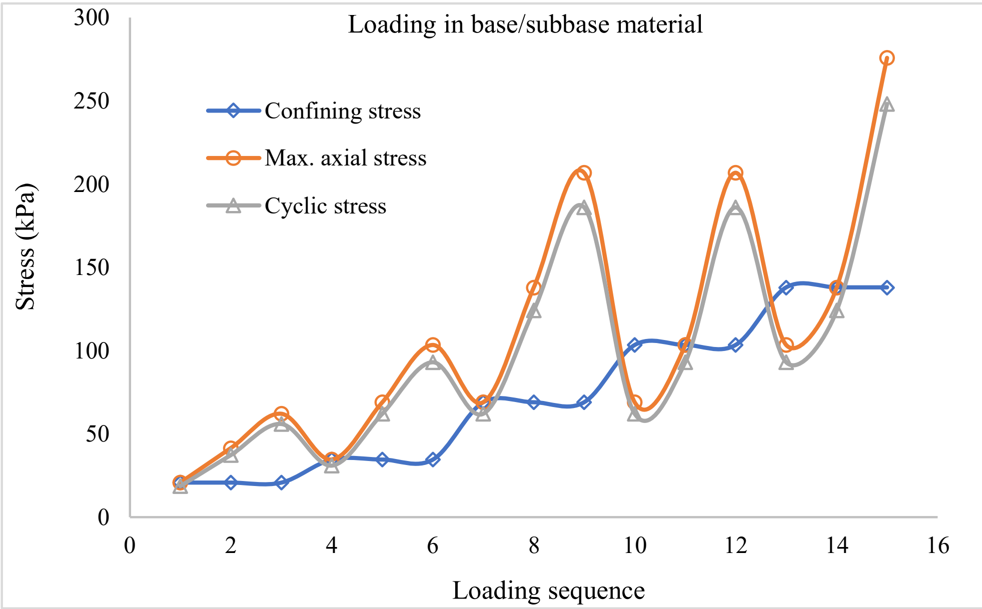


(b)

**Figure 5.13.** Test sequence and loading pattern for (a) soil and (b) aggregates.

The main difference in loading pattern in the two materials (soil and aggregate) lies in confining stress as shown in Figure 5.13. Stress confinement gradually decreases in soil while it increases in aggregate. Further the magnitude of confining stress and axial stress is higher in case of aggregate materials as they are expected to carry higher traffic loads than subgrade soil. Traffic load in the pavement structure gradually decreases from top surface to lower layers as it distributes over larger contact area.

### 5.5.3 Resilient modulus test results

The resilient modulus test as discussed in previous section (see section 5.5.2) was conducted on UGM (subgrade soil and aggregates) to study the stress dependent behaviour of these materials. The resilient modulus of UGMs is considered as a key parameter in the analyses of asphalt concrete pavement [264–266]. UGMs are characterised on the basis of $M_r$ values and it is used to evaluate structural response of the pavement. As discussed earlier, fine grained cohesive soil shows stress softening behaviour subjected to repeated cyclic load. It means, as cyclic stress in the material increases, resilient modulus decreases. However, aggregate materials show stress hardening behaviour and resilient modulus of the material increases with increase in state of stress (cyclic stress). It should be noted that all the soil materials do not exhibit stress softening behaviour. Only fine-grained cohesive soil possesses this peculiar characteristic. The behaviour of other soils (non-cohesive) is different and do not show a fix pattern. Few of the soil (e.g., red soil) show stress hardening behaviour like aggregate materials. However, some of the soils (e.g., fly-ash soil) exhibit a combination of these behaviours (stress softening and stress hardening) with the change in state of stress.

At the other end, irrespective of grade of aggregates used in granular subbase or base layer, it always shows stress hardening behaviour under the application of repeated cyclic load. The cyclic stress applied in soil material starts from a minimum value of 12.4 kPa and increases to 62.0 kPa in 5th loading sequence. Loading sequence 1 to 5 is repeated till 15th sequence.

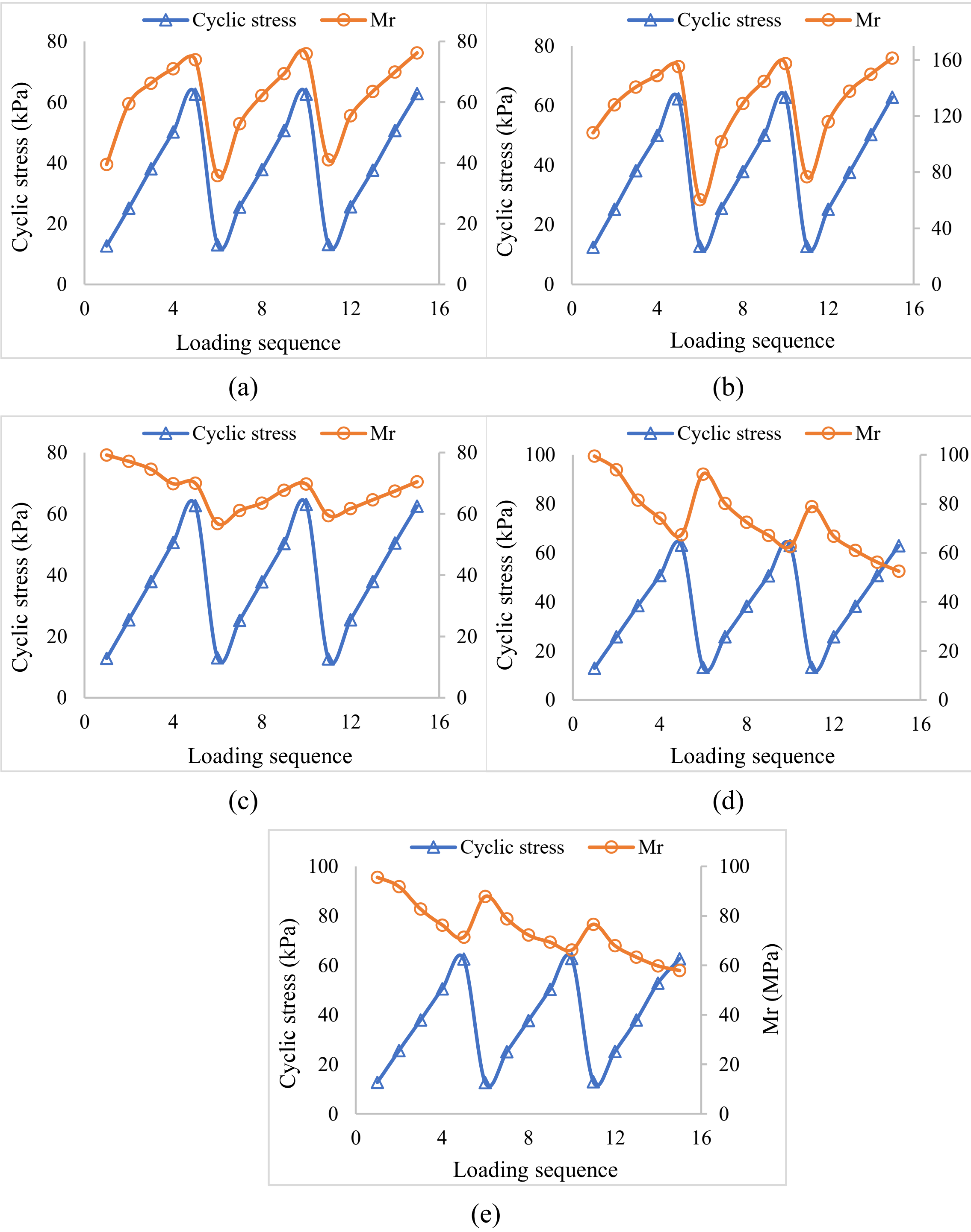


**Figure 5.14.** Stress dependency of resilient modulus with loading sequence (a) red soil 1 (b) red soil 2 (c) fly-ash soil (d) cohesive soil (e) black cotton soil.

However, the cyclic stress in aggregate materials is different in all the sequence of loading. The difference in magnitude of maximum cyclic stress is also high for two materials. The maximum cyclic stress in soil is 62.0 kPa whereas for aggregate materials, it is 248.2 kPa. The response ($M_r$) of various soil materials used in this study in subgrade layer with the change in state of stress (cyclic stress) and loading sequence (excluding conditioning period) is shown in Figure 5.14.

As shown in Figure 5.14 (a) and (b), the response of both the red soil was found similar to that of aggregate materials. The $M_r$ was found to increase with increase in cyclic stress due to the non-cohesive property of the soil. The fine-grained cohesive soil has higher plasticity index which allows for significant plastic flow in the material subjected to repeated cyclic stress. Thus, with the increase in cyclic stress, $M_r$ value decreases as shown in Figure 5.14 (d) and (e) for fine grained cohesive soil and black cotton soil. However, non-cohesive materials do not soften under cyclic stress and plastic flow is insignificant. Any soil which possesses some plasticity and cohesive properties (for example, cohesive soil mixed with fly-ash) may exhibit a combination of stress softening and stress hardening behaviour as shown in Figure 5.14 (c).

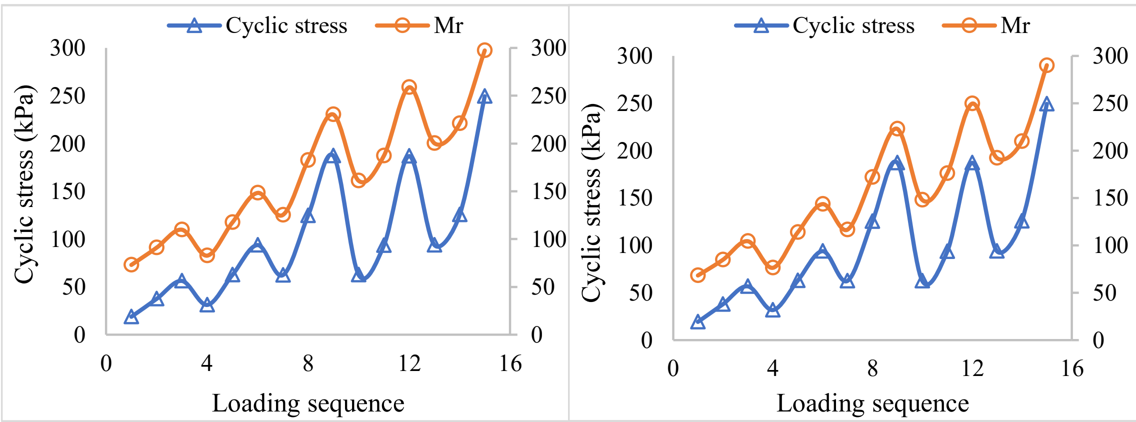


(a) (b)

**Figure 5.15.** Stress dependency of resilient modulus with loading sequence for granular subbase (a) grade V and (b) grade VI.

Similarly, stress dependent behaviour of aggregate materials in granular subbase (grade V and grade VI) was studied and variation of $M_r$ with cyclic stress and loading sequence were plotted as shown in Figure 5.15. It was found that recoverable strain in the aggregate samples decreases with the increase in cyclic stress and thus $M_r$ increases as shown in Figure 5.15. It shows, stiffness of the material increases as cyclic stress increases which is main cause of the stress hardening behaviour of aggregate materials. The $M_r$ of grade V granular subbase material was found marginally higher than grade VI aggregates. This may due to higher percentage of coarser aggregates in grade V granular subbase aggregates. The resilient behaviour of aggregates in granular base (WMM) was also studied as shown in Figure 5.16.

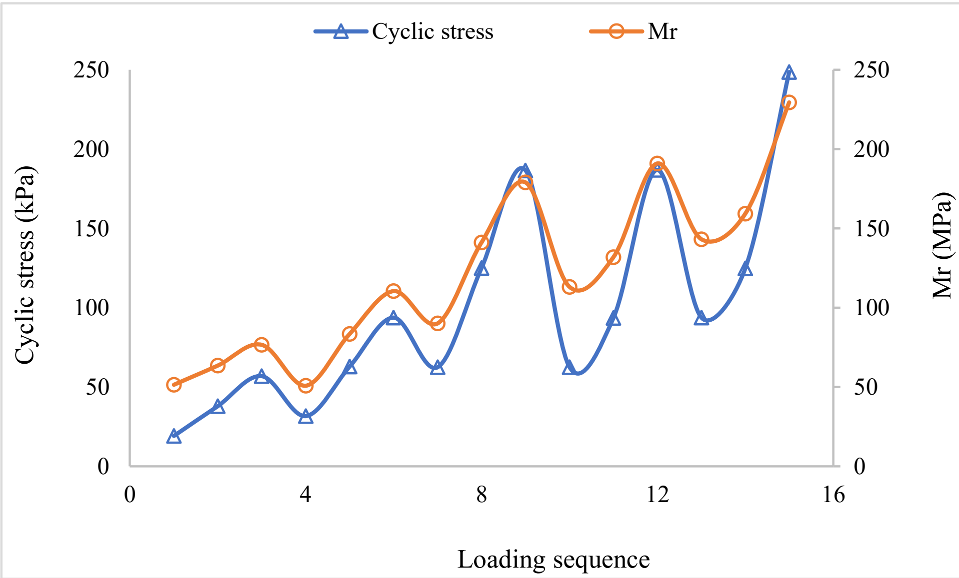


**Figure 5.16.** Stress dependency of resilient modulus with loading sequence for WMM.

The resilient behaviour of aggregates in WMM was similar to granular subbase aggregates as materials and stress level are similar in two cases. These resilient modulus test data were used to model UGMs response in different material models as discussed in following section.

### 5.5.4 Stress dependent material modelling

The bilinear model for subgrade soil, whereas, the k-ϴ model, Uzan model, and the NCHRP model was used to model nonlinear stress dependent behaviour of unbound granular base and subbase layer materials. Deviatoric stress ($\sigma_d$) was first calculated based on axial stress ($\sigma_1$) and confining stress ($\sigma_3$) obtained from the resilient modulus test. Initially, the model constants were given an assumed seed value and based on these parameters, $M_r$ values were obtained for different bulk stresses as obtained from experimental results. The difference in $M_r$ values as predicted from the model and obtained from the triaxial test were estimated and sum of the squares of these differences were determined called as objective function. Constrained optimization process using least square approach was used to minimize this objective function and model parameters were evaluated. It should be noted that, these models (Bilinear, k-ϴ, Uzan, Octahedral shear stress model) are empirical relations between $M_r$ and deviatoric stress or bulk stress or shear stress and thus they cannot be used directly in FE analysis without further assumptions about bulk modulus or Poisson's ratio. So, a constant value of bulk modulus based on average $M_r$ value obtained from all 15 sequence of loading was considered in this analysis.

The stress dependency of $M_r$ was plotted against bulk stress for both experimental and bilinear model in case of subgrade soil and average difference between experimental results and model predicted values are shown in Figure 5.17. Results are shown for the five different soils, red soil-1 (RS-1), Red soil-2 (RS-2), Fly-ash soil (FAS), Fine-grained cohesive soil (CS), and Black cotton soil (BCS). The silt content in red soil were relatively higher which made it less cohesive. Fly-ash soil collected nearby railway tracks was found to have both fly-ash and cohesive soil characteristics. However, black cotton soils are purely cohesive soil and thus Bilinear model are best fit for fine-grained cohesive as well as black cotton soil.

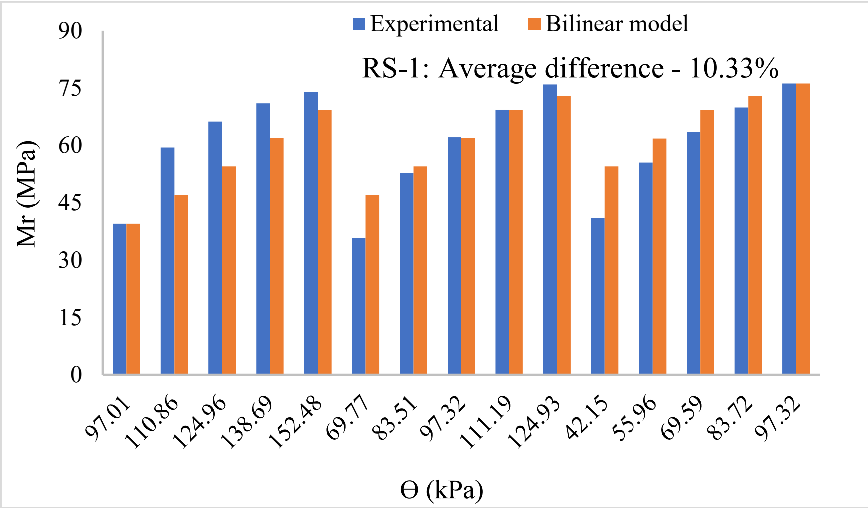


(a)

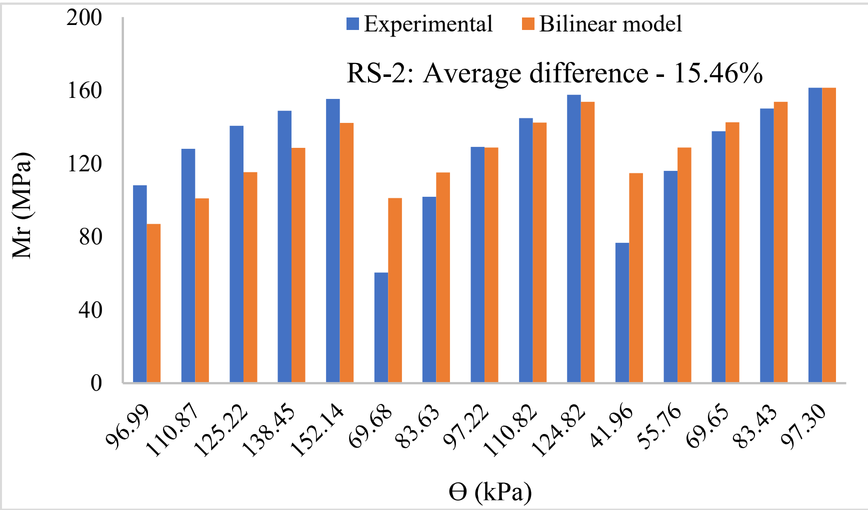


(b)

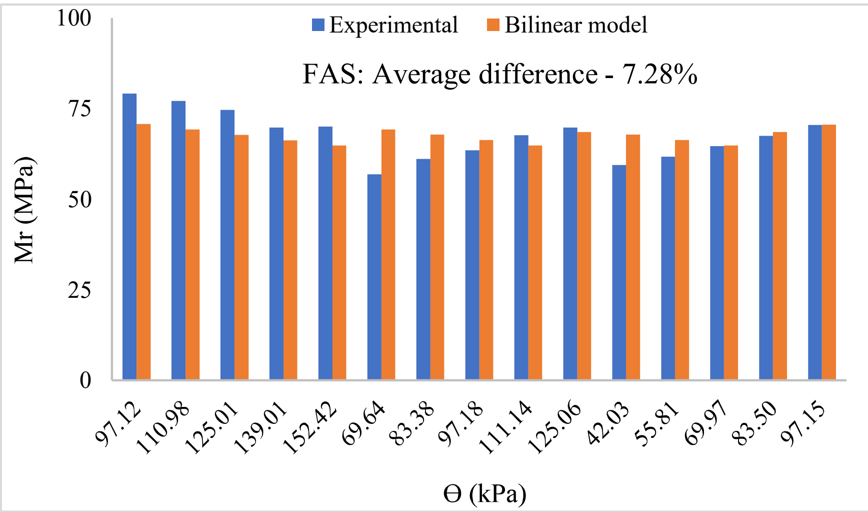


(c)

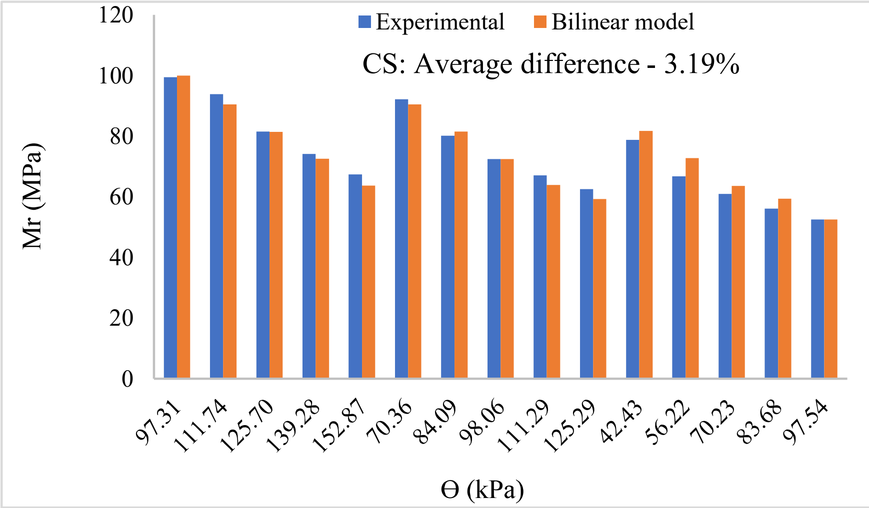


(d)

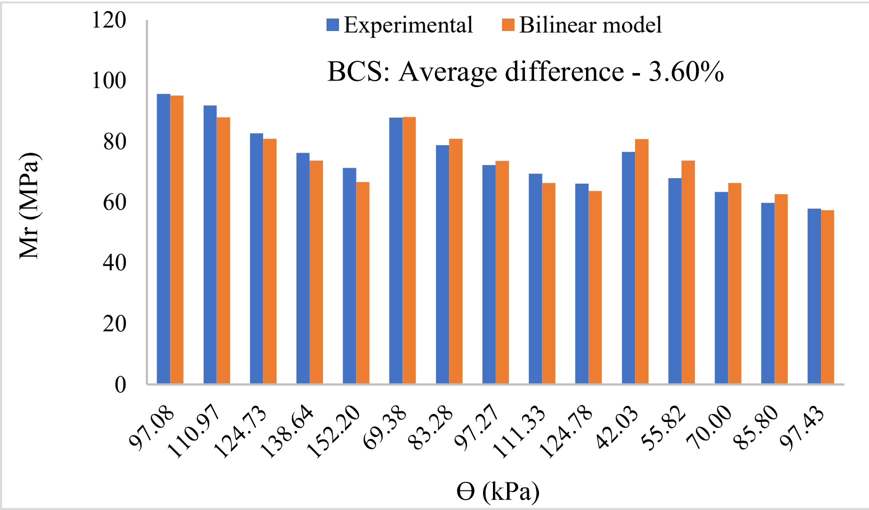


(e)

**Figure 5.17.** $M_r$ vs ϴ, fitted with experimental and Bilinear model for (a) Red soil-1 (b) Red soil-2 (c) Fly-ash soil (d) Cohesive soil and (e) Black cotton soil.

The average difference in $M_r$ values determined experimentally and predicted from Bilinear model is highest for red soil (both RS-1 and RS-2) and lowest for cohesive soil. It shows the usefulness of the Bilinear model to fit the $M_r$ data for cohesive soils. This model is not suitable for silty soils or other non-cohesive type of soils where some other models must be considered. Resilient modulus data are based on recoverable strains in the material. These strains are function of axial stress applied to the material. To study the variation of the axial resilient strain in the soil sample as determined from repeated load triaxial testing, it was plotted against axial stress as shown in Figure 5.18.

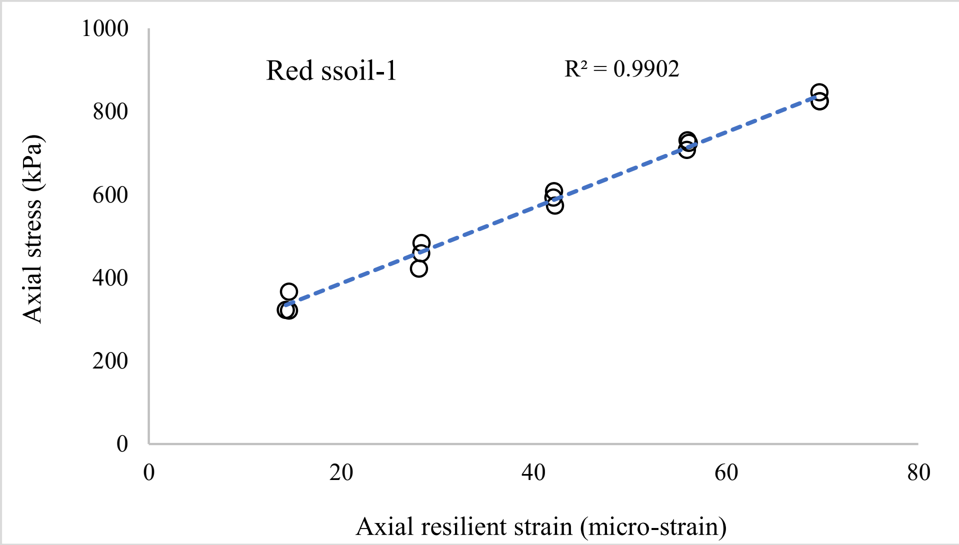
Red ssoil-1
R² = 0.9902
Axial stress (kPa)
0
200
400
600
800
1000
0
20
40
60
80
Axial resilient strain (micro-strain)

(a)

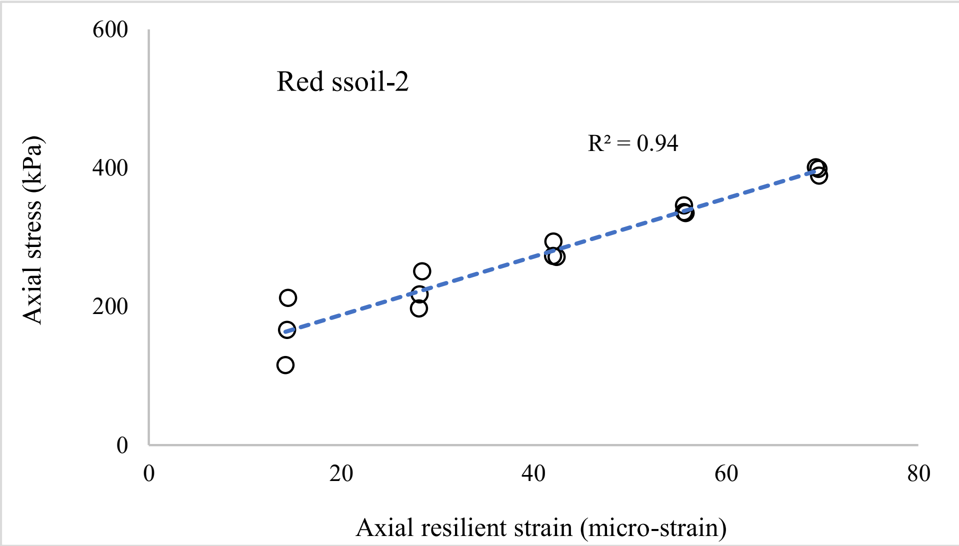
Red ssoil-2
R² = 0.94
Axial stress (kPa)
0
200
400
600
0
20
40
60
80
Axial resilient strain (micro-strain)

(b)

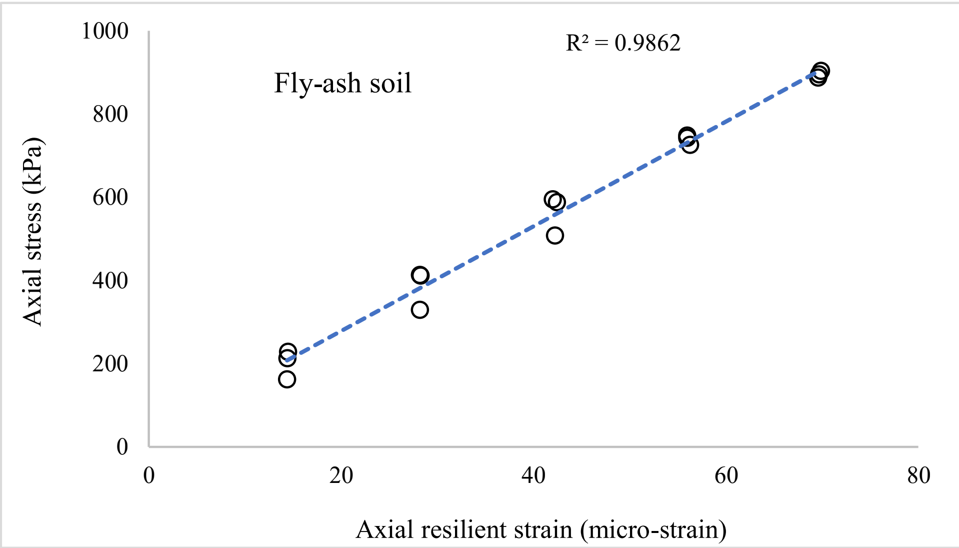
R² = 0.9862
Fly-ash soil
Axial stress (kPa)
0
200
400
600
800
1000
0
20
40
60
80
Axial resilient strain (micro-strain)

(c)

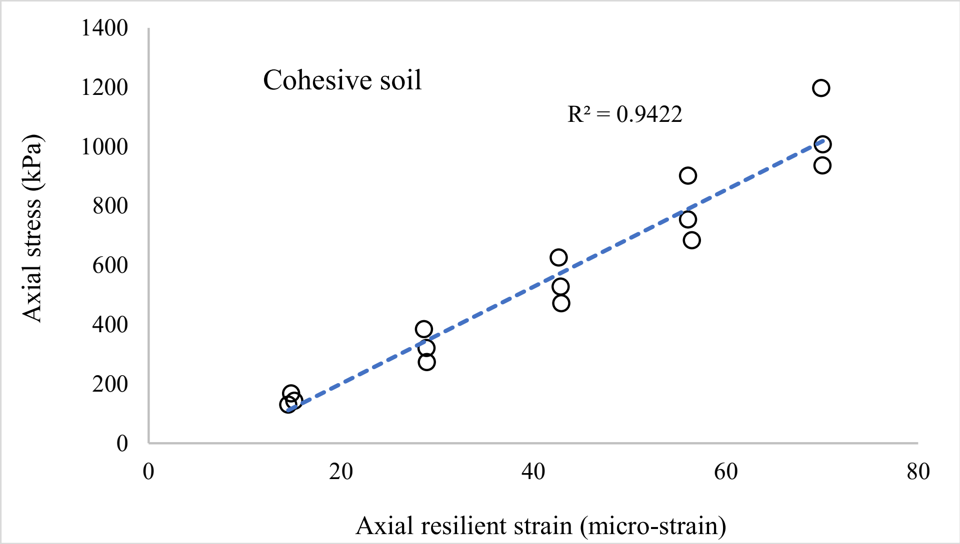


(d)

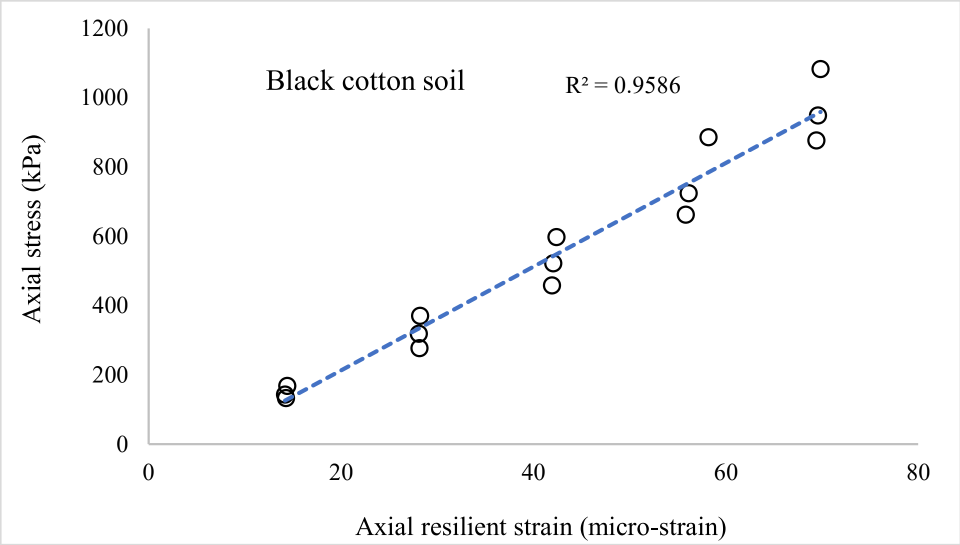


(e)

**Figure 5.18.** Variation of axial resilient strain with applied axial stress for (a) Red soil-1 (b) Red soil-2 (c) Fly-ash soil (d) Cohesive soil and (e) Black cotton soil.

The resilient strain in the sample was found to increase with the increase in axial stress value. It was found that, irrespective of the soil type, there exists linear relation between resilient strain and axial stress in the soil material. The coefficient of determination ($R^2$) value varied between 0.94 to 0.99, which indicates the good linear fitting of these experimental data. The model constants for Bilinear model obtained from constrained optimization process is shown in Table 5.7.

**Table 5.7.** Model parameters for soil used in the present study

| Type of soil | Model parameters | | | |
|---|---|---|---|---|
| | $k_1$ (MPa) | $k_2$ (kPa) | $k_3$ | $k_4$ |
| Red soil – 1 | 69.98 | 29.66 | -0.53 | -0.23 |
| Red soil – 2 | 150.42 | 36.06 | -1.00 | -0.55 |
| Fly-ash soil | 65.53 | 21.71 | 0.10 | -0.14 |
| Cohesive soil | 73.09 | 14.34 | 0.65 | 0.49 |
| Black cotton | 92.43 | -22.00 | 0.51 | 0.44 |

The breakpoint modulus ($k_1$) is a representative parameter of material stiffness. The higher is the $k_1$ value, higher will be the $M_r$. As shown in Table 5.7, $k_1$ is highest for red soil-2 and lowest for fly-ash soil, which indicates the highest $M_r$ value for red soil-2 and lowest $M_r$ for fly-ash soil.

### 5.5.5 Hypo-elastic material modelling

Elastic constants (elastic modulus and Poisson's ratio or bulk modulus) are basically functions of strain invariant ($I_1$, $I_2$, *and* $I_3$), where bulk modulus is assumed constant in the analysis. This assumption makes the relation between volumetric stress and volumetric strain linear as per Hooke's law. This is an important assumption in the hypo elastic modelling. The first strain invariant ($I_1$) denotes volumetric strain in the sample, and it is given as the following constitutive relation:

$$I_1 = \varepsilon_{vol} = \varepsilon_{11} + \varepsilon_{22} + \varepsilon_{33} \tag{5.8}$$

$$\sigma_{vol} = K \times \varepsilon_{vol} \tag{5.9}$$

where, $\varepsilon_{11}, \varepsilon_{22}, and\ \varepsilon_{33}$ are principal strains in the material along the principal directions and $K$ is bulk modulus assumed constant.

The stress dependency of $M_r$ for aggregates in base and subbase layers were also determined using repeated load triaxial testing and experimental data were fitted with k-θ model, Uzan model, and NCHRP model. The $M_r$ data were plotted against bulk stress to study the best fit model as shown in Figure 5.19.

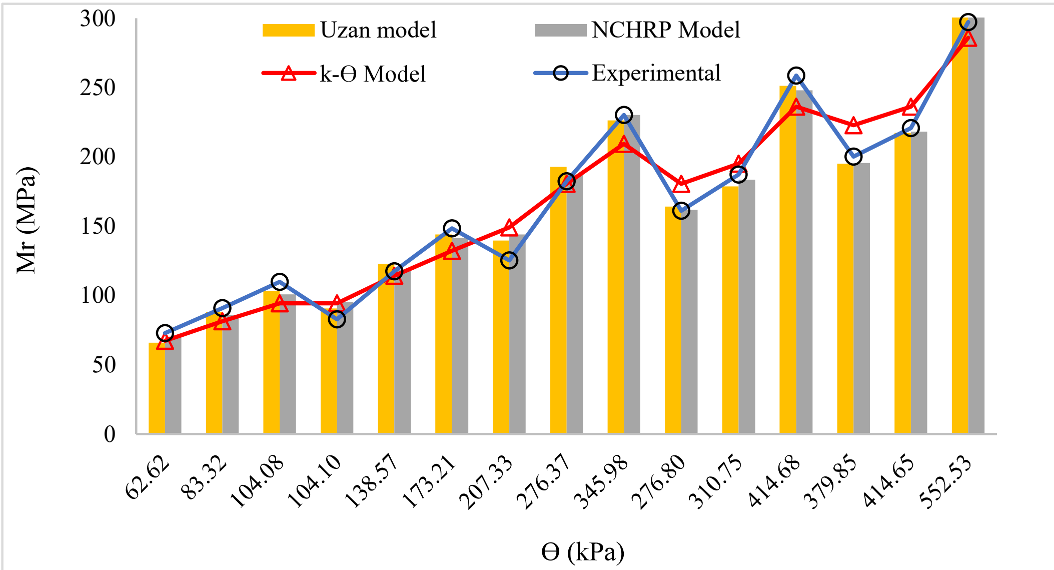


(a)

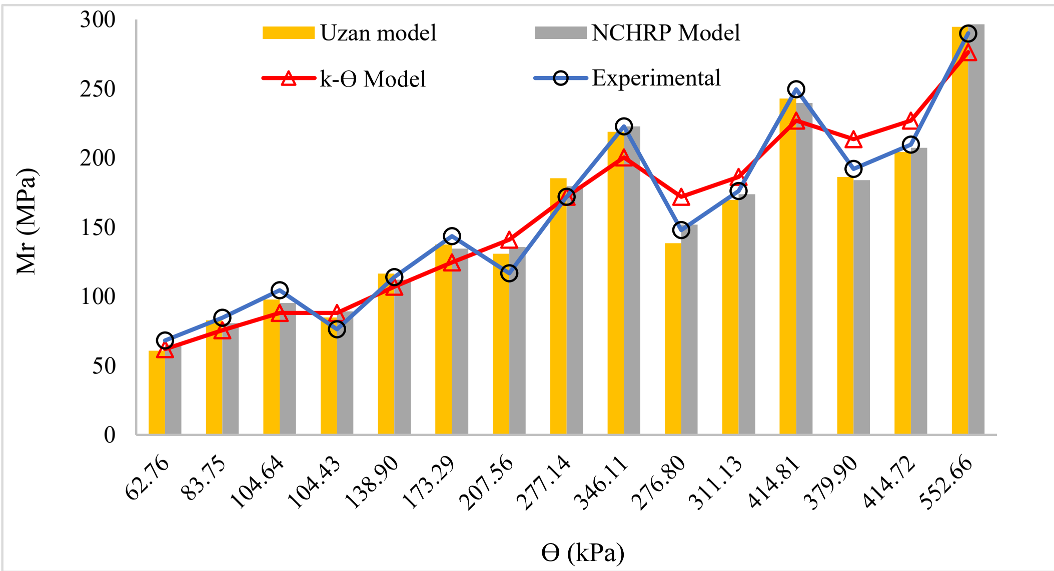


(b)

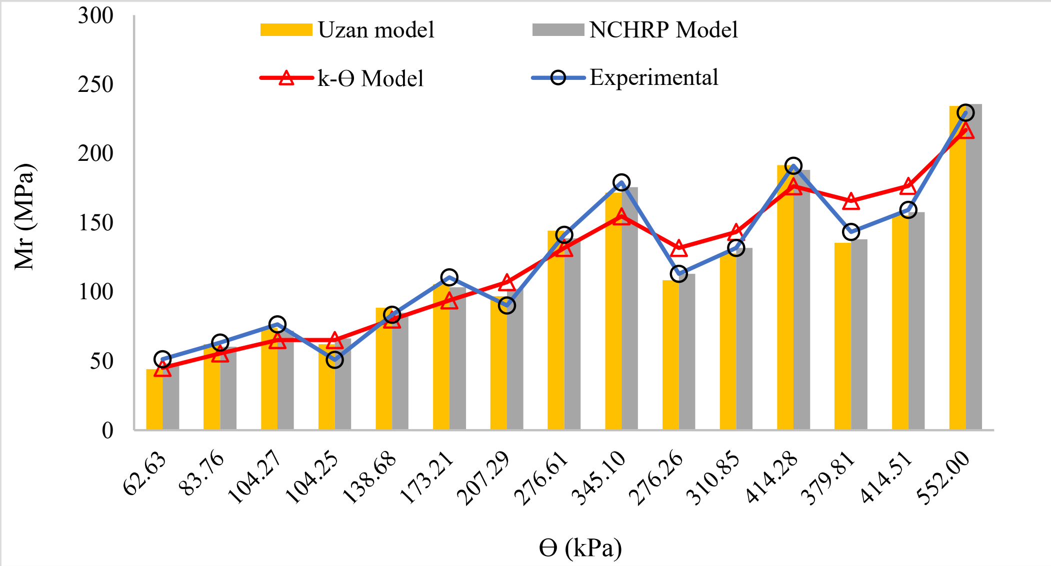


(c)

**Figure 5.19.** Variation of $M_r$ with bulk stress for GSB (a) grade V (b) grade VI and (c) WMM.

Different models (k-Θ model, Uzan model, and NCHRP model) were used to fit $M_r$ test data and compared with experimental results. It was found that, NCHRP model best fits the stress dependent response of $M_r$ in unbound granular layers (base and subbase layers) whereas, k-Θ model predicts these responses least reliably. Since, the NCHRP model considers the role of octahedral shear stress along with bulk stress in the determination of resilient modulus, it predicts $M_r$ value more reliably. However, the k-Θ model only considers bulk stress dependency of $M_r$, a significant difference with experimental results is observed. The Uzan model considers the deviatoric stress instead of octahedral shear stress in $M_r$ model, which gives close result to NCHRP model. It can be concluded that, both Uzan model and NCHRP model can be used to predict stress dependent behaviour of UGMs reliably in base and subbase layers. The resilient modulus value is determined experimentally using resilient strain and deviatoric stress. The resilient strain determined from repeated load triaxial test for UGMs in base and subbase layers were plotted against applied axial stress as shown in Figure 5.20.

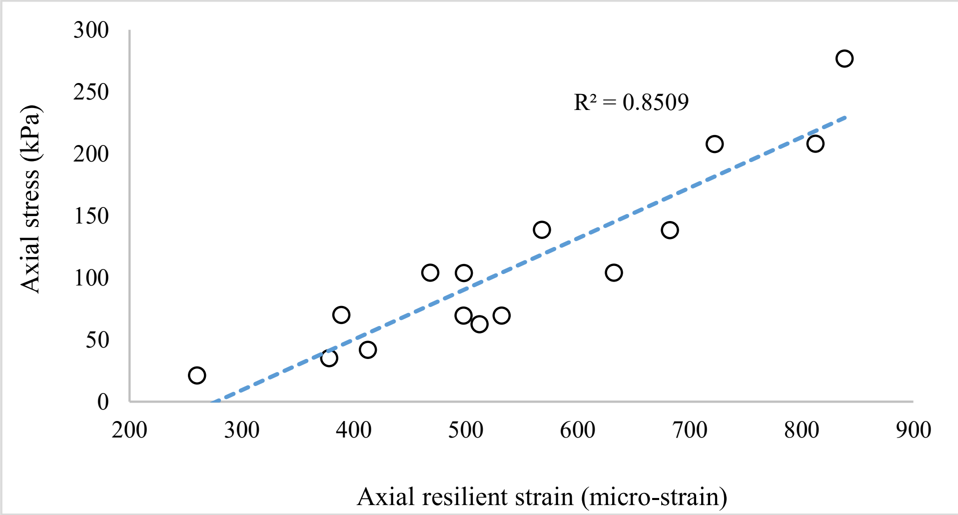


(a)

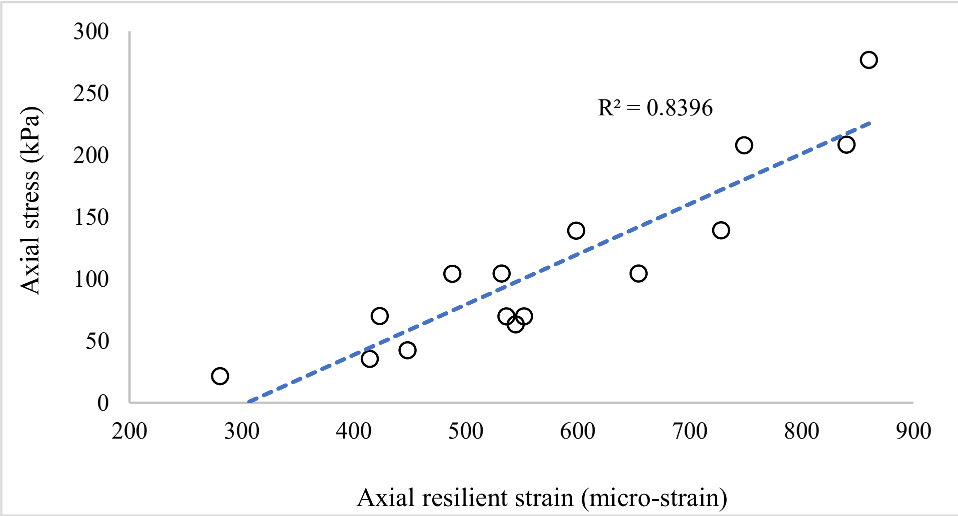


(b)

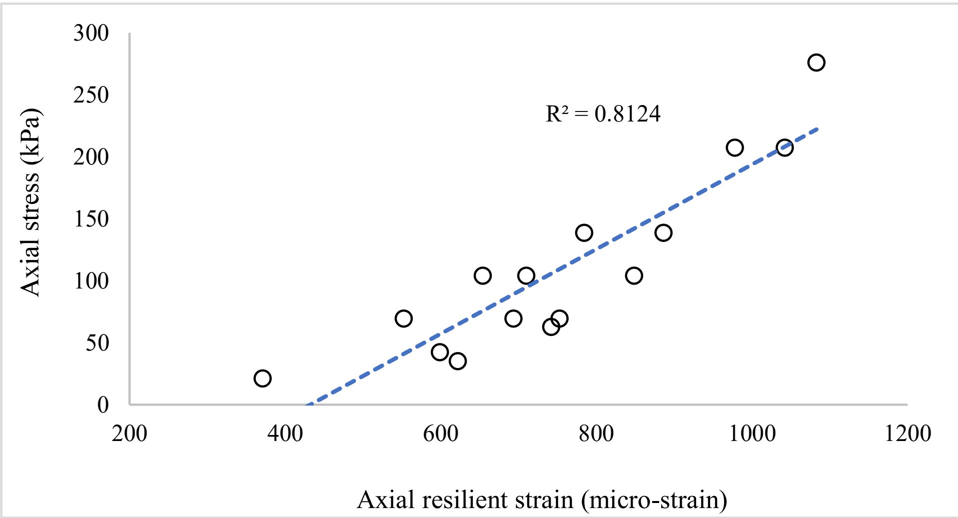


(c)

**Figure 5.20.** Variation of resilient strain with axial stress for GSB (a) grade V (b) grade VI and (c) WMM.

The similar trend of linear relationship between resilient strain and axial stress as found in case of soil material was not found for aggregates in base and subbase layer. The $R^2$ values for linear fit were found relatively lesser. Thus, it can be concluded that, resilient strains in aggregate materials are not linearly proportional to applied stress.

## 5.6 Summary

The mechanistic methods used in the analysis of layered pavement systems under repeated traffic loading, various layers in the pavement are considered as homogeneous, isotropic, and linear elastic. It works reasonably well, if the subgrade layer behaves as linear elastic system under static loading. However, in real field conditions, these heterogeneous layers behave far from ideal conditions and subjected to dynamic loading. Pavement materials, the fine-grained soil in the subgrade layer and aggregates in untreated base/subbase layers shows stress dependent nonlinear behaviour under repeated loading conditions. This nonlinear behaviour of UGMs is generally characterized by resilient modulus test using triaxial compression testing. These material characteristics of UGMs need to be considered in FE based mechanistic pavement analysis methods to predict more accurately the resilient response for a reliable pavement design.

Various design agencies throughout the world are shifting their pavement design approach toward mechanistic empirical. AASHTO developed AASHTOWare software based on mechanistic empirical pavement design guide. It allows design engineers to leverage advanced material mechanics like consideration of nonlinear stress dependent properties of UGMs which predicts pavement response more accurate and gives a higher degree of reliability in asphalt pavement design. However, these advancements in material mechanics as an input parameter are still missing in many developing countries design guidelines including India. Currently, IITPAVE, based on linear elastic properties of materials in various layers is used as asphalt pavement analysis and design tool in India. As discussed earlier, elastic properties of materials often underestimate or overestimate its strength and may result in uneconomical pavement design. So, consideration of more realistic material behaviour in pavement analysis will help to reach an optimized design. It will require extensive experimental and field testing on UGMs to study the material behaviour under repeated cyclic loading conditions. Additionally, advancement in existing analysis tool is required to consider stress dependent nonlinear material response. FE based asphalt pavement model has been developed to consider stress dependency of UGMs as input parameter in pavement analysis.

To study stress dependent behaviour of UGMs, the resilient modulus test was conducted on five different soils for subgrade layer, aggregates for GSB grade V and grade VI used as drainage cum filter layer in subbase layer, and WMM as base layer. In resilient modulus test, sample is subjected to repeated triaxial loading with different stress level in different sequence of loading. It was found that, various soil materials have different response to applied cyclic loading. Some of them (red soil-1 and red soil-2) exhibits stress hardening ($M_r$ increases with increase in cyclic stress) behaviour, however some of them (fine-grained cohesive soil and black cotton soil) shows stress softening ($M_r$ decreases with increase in cyclic stress) behaviour. A few of them like fly-ash soil exhibits dual characteristics, they show stress softening behaviour initially for a few sequences of loading and after that stress hardening behaviour of rest of the loading sequence. However, aggregate materials used in subbase and base layers exhibits unidirectional stress hardening response.

The resilient modulus test data were fitted to different material models used to explain nonlinear stress dependent response of UGMs. It was found that, the NCHRP model best fits the predicted $M_r$ data of base and subbase layers as difference between predicted and experimental $M_r$ values were found lowest. However, significant difference in $M_r$ values obtained experimentally and predicted from k-Θ model was observed. Since, the k-Θ model is based on bulk stress parameter only, these variations are expected. The NCHRP model considers the effect of octahedral shear stress also on the $M_r$ of the aggregate materials, it is able to predict stress dependency of $M_r$ more reliably. The Uzan model which considers deviatoric stress and bulk stress as the independent parameter and $M_r$ as dependent parameter, is capable of predicting resilient response of aggregate materials reliably, however with lesser accuracy than NCHRP model.

The resilient response of soil material was modelled using Bilinear model. It was found that, Bilinear model can be used to fit experimental data of cohesive soil with higher degree of accuracy than other types of soil. The average difference in $M_r$ values as obtained experimentally and predicted from Bilinear model for cohesive soil was found to vary between 3-4%. However, this variation was significantly higher (7-11%) for other soils (red soil and fly-ash soil) which are not purely cohesive in nature.

Finally, these material properties of asphalt mixes (as obtained in chapter 4) and UGMs (as obtained in this chapter) were used in the FE model to define behaviour of materials in various layers of the asphalt pavement. In the next step, the FE model was used to study effect of overloading conditions, high temperature conditions, air voids in the mixes, base layer stabilization, and layer thickness on the structural response and life of asphalt pavement as discussed in detail in the next chapter. Since, overloading and increasing temperature over the years in a tropical country like India has been the rising concern; so, this study considers the effect of these crucial parameters on pavement response. The measures like base layer stabilization and increase in suitable layer thickness to improve deteriorating effect of overloading and increasing temperature has been considered.